Journal of Korean Society of
Coastal and Ocean Engineers
Vol. 9, No. 2, pp. 63~73, June 1997

A Numerical Tidal Model for the Southeast Asian Seas
南東 아시아 海域의 潮汐 數値 模型

Byung Ho Choi*, Duk Gu Kim** and Dong Hoon Kim**
崔秉昊* · 金德九** · 金東勳**

Abstract The tidal propagation for the Southeast Asian Seas is described via a high-resolution, two-dimensional hydrodynamic model by the equilibrium tide and co-oscillating tide at the Straits. Computed tidal distributions of four major semidiurnal tides (M_2, S_2, K_2, N_2) and four major diurnal tides (K_1, O_1, P_1, Q_1) are presented and results are also compared with coastal observations archived in IHO global tidal data base (Canadian Marine Environmental Data Service) and existing tidal charts including Schwiderski GOTD(Global Ocean Tidal Data) maps.

Keywords : tidal model, South China Sea

要 旨 : 本 硏究에서는 起潮力項이 포함된 1/12°×1/12°의 解像度를 갖는 2次元 潮汐模型을 사용하여, 동남 아시아 전역에 대한 4개의 半日週潮(M_2, S_2, K_2, N_2)와 4개의 日週潮(K_1, O_1, P_1, Q_1)의 분포를 산정하였다. 산정 결과들은 관측 자료들과의 비교되었으며 기존의 Schwiderski의 潮汐圖 및 기존의 일부 海域만을 포함하는 潮汐圖와 비교 검토되었다.

핵심용어 : 조석모형, 남중국해

1. INTRODUCTION

In this study, tidal propagation for the Southeast Asian Seas covering the South China Sea, the Java Sea, the Celebes Sea and the Sulu Sea are inverstigated. In Fig. 1 the modelled region, bounded by Vietnamese coast, Malaysia and Strait of Malacca to west, the Taiwan Strait to north, the Bashi Strait, the east openings of the Celebes Sea and the Flores Sea to east and Sumatra, Java and Lesser Sunda Islands to south, lies the South China Sea and the regional seas forming large semi-enclosed shallow seas. It is connected to the Indian Ocean by the Malacca Strait, the Sunda Strait and several small openings between the Java, Bali, Sumbawa and the Flores Islands. The Taiwan Strait is shallower connection to the East China Sea and two openings of the Bashi Strait and the east of the Celebes Sea are connected to the Pacific Ocean. The east of the Flores Sea connected to the Banda Sea was also treated as eastern model boundary.

Thus the model coverage is considerably large semi-enclosed sea area from 95° to 125° east longitude and from 7° south latitude to 25° north latitude. The modelled region was divided into finite-difference mesh system, each mesh element being 5 minutes in latitute and 5 minutes in longitude which is one to two mesh refinement of previous tidal model of Choi and Ko (1994) covering more wider region from the Kamchatka to the South China Sea (see tidal distribution of the East Asian Marginal Seas in Fig. 2).

The tides in the South China Sea and the Java Sea area has been previously modelled with different region

*成均館大學校 土木工學科(Department of Civil Engineering, Sung Kyun Kwan University, Suwon 440-746, Korea)
**成均館大學校 韓國海洋硏究所 學硏課程(Sung Kyun Kwan University KORDI Joint Graduate Program on Coastal and Ocean Engineering)

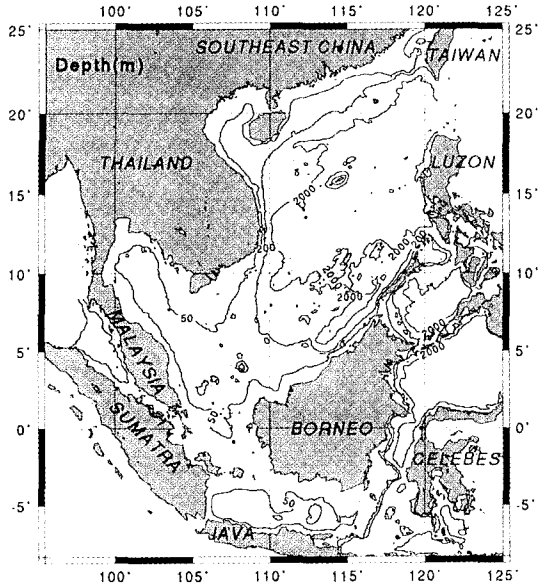

Fig. 1. Bathymetric map of the South China Sea and the Java Sea.

of interests with varying degree of reproduction (Thuy, 1968; Ye and Robinson, 1983; Roos, 1989; Rahman *et al.*, 1990). As multiyear altimeter dataset from the TOPEX/POSEIDON mission were available, improvement of global tidal model by empirical method using data only (Schrama and Ray, 1994; Mazzega and Berge, 1994), assimilation using data and hydrodynamic modeling (Egbert *et al.*, 1994) and hydrodynamic modelling (Le Provost *et al.*, 1994) were performed. A model by DHL (Roos, 1989) was focussed on coastal zone of the Java Sea with nested grids over the similar model boundary to our present model but northern boundary was limited to middle part of the South China Sea. A global model by Le Provost *et al.* (1994) has fine resolution of FEM meshes over the present modeling region with reproduction of eight constituents for removal of tides from T/P altimeter data.

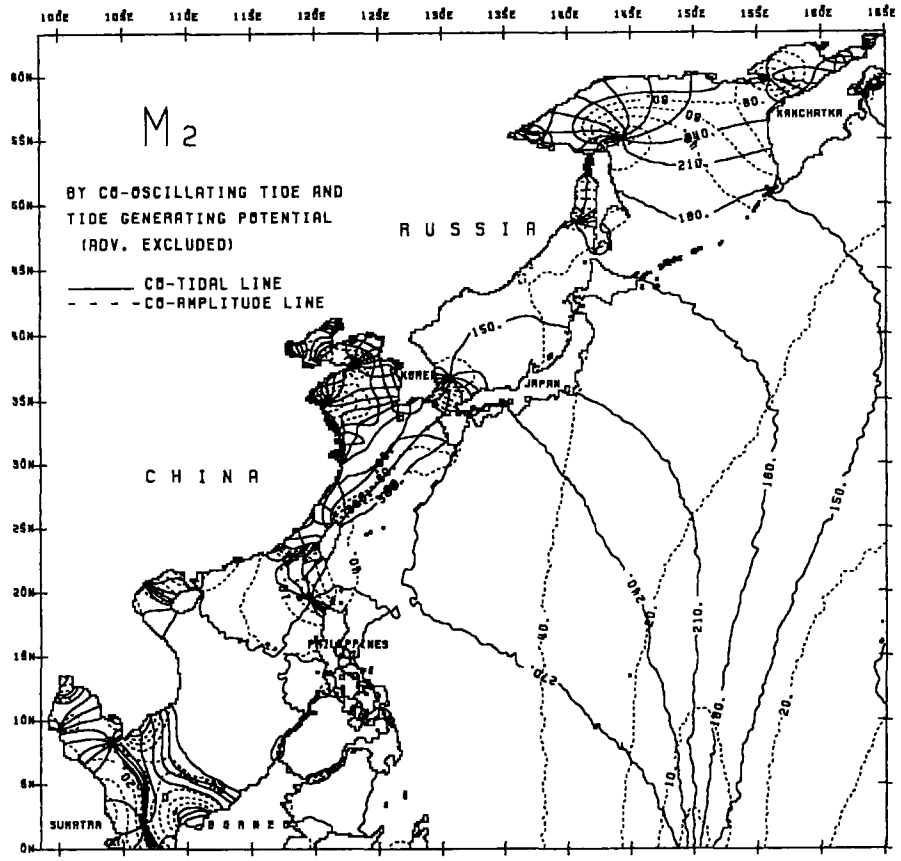

Fig. 2. M_2 tidal distribution of the East Asian Marginal Seas (Choi and Ko, 1994).

We also formulated a fine mesh two-dimensional hydrodynamic model utilizing the DBDB5 (Digital Bathymetric Data Base 5 minutes).

2. THE HYDRODYNAMIC NUMERICAL MODEL

The vertically integrated equations for ocean tides, in spherical coordinates, incorporate a quadratic law of bottom friction, nonlinear terms and include the direct influence of the tide-generating potentials terms, they take the follwing form:

$$\frac{1}{R\cos\phi}\left\{\frac{\partial}{\partial\chi}(HU)+\frac{\partial}{\partial\phi}(HV\cos\phi)\right\}+\frac{\partial\xi}{\partial t}=0 \qquad (1)$$

$$\frac{\partial U}{\partial t}+\frac{U}{R\cos\phi}\frac{\partial U}{\partial\chi}+\frac{V}{R\cos\phi}\frac{\partial(U\cos\phi)}{\partial\phi}-\frac{UV\tan\phi}{R} = 2\omega\sin\phi V-\frac{g}{R\cos\phi}\frac{\partial(\alpha\xi-\beta\xi_0)}{\partial\chi}-\frac{k_b U\sqrt{U^2+V^2}}{H} \qquad (2)$$

$$\frac{\partial V}{\partial t}+\frac{U}{R\cos\phi}\frac{\partial V}{\partial\chi}+\frac{V}{R}\frac{\partial V}{\partial\phi}+\frac{U^2\tan\phi}{R} = -2\omega\sin\phi U-\frac{g}{R}\frac{\partial(\alpha\xi-\beta\xi_0)}{\partial\phi}-\frac{k_b V\sqrt{U^2+V^2}}{H} \qquad (3)$$

where the notation is as follows:

χ, ϕ : east-longitude and north-latitude, respectively;

t : time;

ξ : elevation of sea surface;

h : undisturbed depth of water;

$H=h+\xi$: total depth of water;

R : radius of the Earth;

ω : angular speed of the Earth's rotation;

g : acceleration due to gravity;

ξ_0 : the equilibrium tide;

α, β: parameters to account for the tidal potential, earth tide, and loading tide;

U, V: components of the depth-mean current given by

$$U=\frac{1}{h+\xi}\int_{-h}^{\xi}u(z)\,dz,\quad V=\frac{1}{h+\xi}\int_{-h}^{\xi}v(z)\,dz \qquad (4)$$

$u(z)$, $v(z)$: components of current in the direction of increasing χ and ϕ, respectively, at a depth z below the undisturbed sea surface;

k_b : the coefficient of quadratic bottom friction and taken as uniform (0.0025) for the present computation.

Boundary conditions for the model are no flow normal to the coast and specified elevations for co-oscillating tides along the Straits and the openings with values taken from Schwiderski's Global Ocean Tidal Data maps and tidal constants from IHO global tide data base.

Another predominant forcing for the model is the tide generating potential, the earth tide, and ocean loading. Assuming the earth to be elastic, the first two forcing terms are usually (e.g., Schwiderski (1978)) expressed as $\beta\xi_0$, where

$$\beta=1+k+h \qquad (5)$$

and k, h are Love numbers relating the body earth tide (and associated perturbations) to the potential. Although the values k=0.3 and h=0.61 are often assumed for all constituents, we have used the frequency dependent values calculated by Wahr (1981), which are recommended by the TP satellite Tidal Committee and summarized in Table 1.

The equilibrium tide for constiuent n, namely ξ_{on}, is expressed as (Cartwright (1978), Schwiderski (1978))

$$\xi_{on}=H_n\cos^2\phi\cos(\sigma_n t+2\lambda+V_n) \text{ for semi-diurnals} \qquad (6)$$

$$=H_n\sin 2\phi\cos(\sigma_n t+\lambda+V_n) \text{ for diurnals} \qquad (7)$$

where the amplitudes H_n are given in Tabel 1; σ_n is the frequency and V_n is the astronomical argument. For the present runs, we have arbitrarily chosen V_n=0 for all

Table 1. Love numbers and tidal potential amplitudes.

constituent	K	h	H_n
M_2	0.302	0.609	0.24408
S_2	0.302	0.609	0.11355
K_2	0.302	0.609	0.04674
N_2	0.302	0.609	0.03090
K_1	0.256	0.520	0.14246
O_1	0.298	0.603	0.10128
P_1	0.287	0.581	0.04713
Q_1	0.298	0.603	0.01940

constituents.

In accordance with the findings of Ray and Sanchez (1989), the ocean loading tide (the deformation of the elastic earth due to the redistribution of mass in the ocean tide) is approximated by assuming it to be in phase with the ocean tide and a fixed percentage of that value. Following the TP Satellite Tidal Committee and Foreman *et al* (1992), we compromised between the suggested values of 0.940 and 0.953 (Ray and Sanchez, 1989) for the diurnal and semi-diurnal constituents by setting α=0.946 for all constituent.

A finite difference grid with 1/12° resolution were formulated using 5 minutes bathymetric dataset. Provision has been made in the model for the future inclusion of cyclone simulation although the present study is restricted to tidal phenomena. Equation (1~3) were solved using finite difference scheme, which advances ξ, U, V over the entire grid network at time t to the values of those variables at time $t+\Delta t$ is explicit: employing central space differences and a combination of forward and backward time difference in the manner described by Flather and Heaps (1975) and Choi (1980).

With both semi-diurnal and diurnal forcing, each model was started from the state of rest and run for 20 tidal cycles. Time series plots of elevations at random locations showed that the model had reached dynamic equilibrium after that time. Using half hourly or hourly values over the last cycle, Fourier analyses were then used to calculate amplitudes and phases as function of (χ, ϕ).

3. MODEL RESULTS

A series of numerical experiments was carried out for four diurnal and four semi-diurnal tides to simulate the tidal distribution at various coastal locations in order to search satisfactory agreement with existing tidal charts of the region. Figs. 3 to 6 and Figs. 7~10 show the model-generated charts of semi-diurnal (M_2, S_2, K_2, N_2) and diurnal (K_1, O_1, P_1, Q_1) tides respectively. General patterns of model-generated co-tidal and co-amplitude lines of the M_2 and K_1 tides are in general agreement with existing tidal charts, but locally there were some discrepancies. As seen by Fig. 3, the M_2 tide progress from the Pacific Ocean through the Bashi Strait (between Taiwan and Luzon) and southwestwards through the main part of the Sea, then the Gulf of Tonkin and propagation into the Gulf of Thailand.

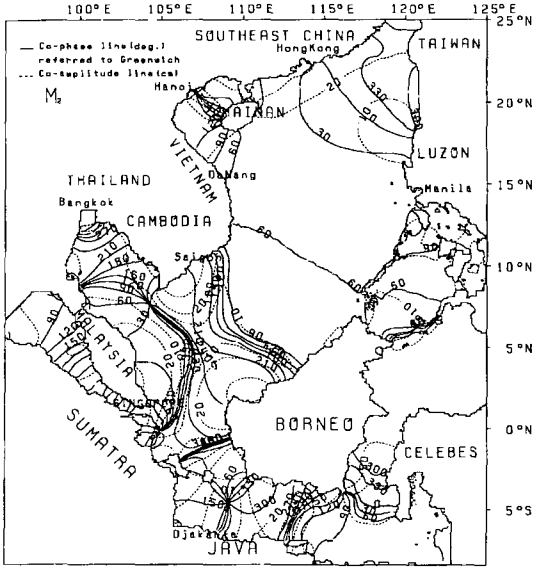

Fig. 3. Computed tidal charts of the M_2 tides for the South China Sea and the Java Sea.

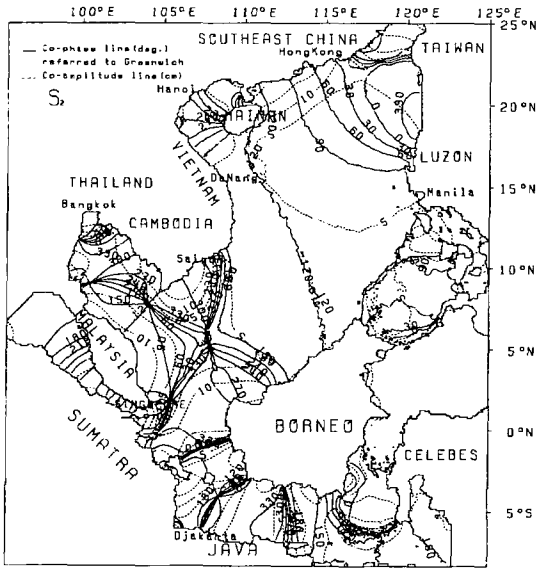

Fig. 4. Computed tidal charts of the S_2 tides for the South China Sea and the Java Sea.

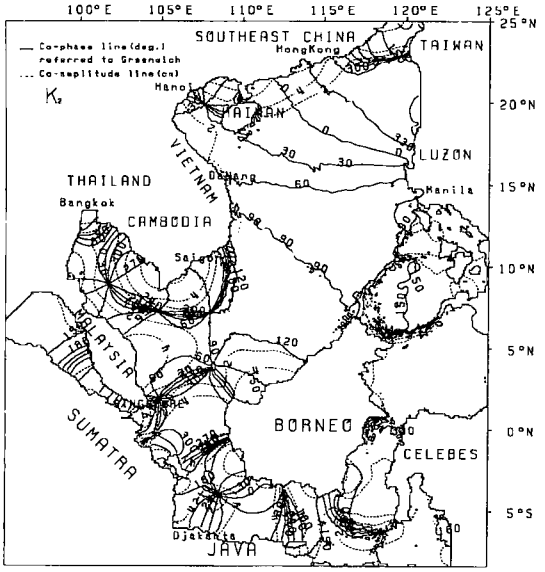

Fig. 5. Computed tidal charts of the K_2 tides for the South China Sea and the Java Sea.

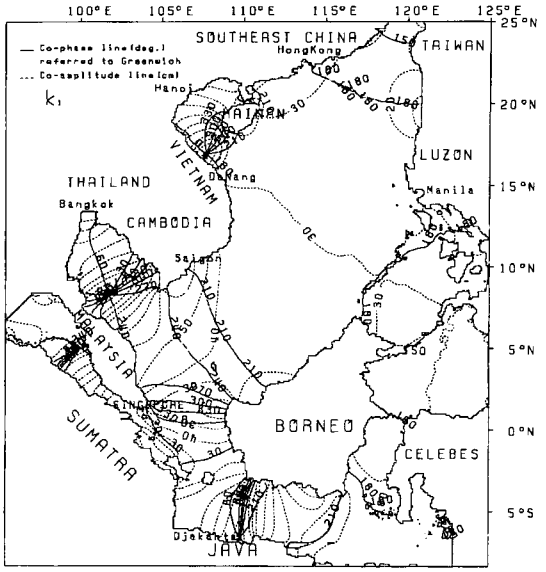

Fig. 7. Computed tidal charts of the K_1 tides for the South China Sea and the Java Sea.

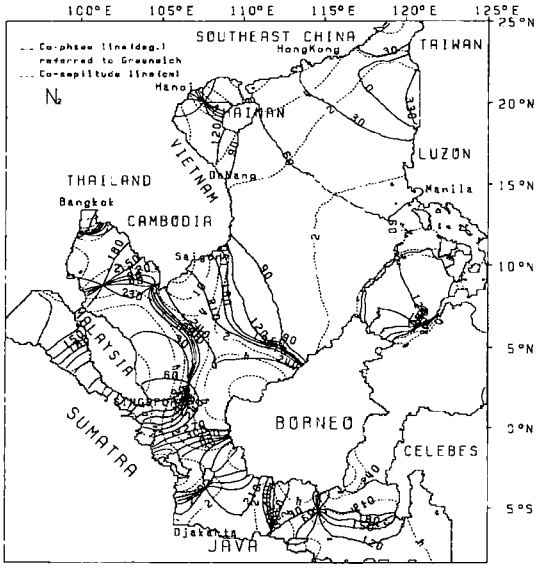

Fig. 6. Computed tidal charts of the N_2 tides for the South China Sea and the Java Sea.

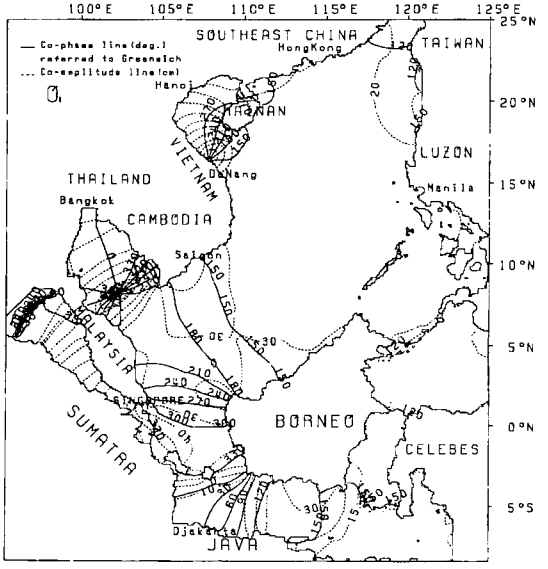

Fig. 8. Computed tidal charts of the O_1 tides for the South China Sea and the Java Sea.

In addition to this tidal propagation, tide entering from the Indian Ocean through the Malacca Strait propagate to the Singapore Strait forming a amphidromic system at the east of the Kepulauan Lingga. Tides in the Java Sea comes from the Pacific Ocean through the Makassa Strait and propagate westwards and meet southward propagation of tide from the lower South China Sea thus forming nodal lines between Bangka Island and the Borneo. Existence of two amphidromic points in the Java Sea are coincide with Schwiderski's result and there is agreement of existence of an amphidromic points in the east of Kepuauan Lingga between the model results and M_2 inverse solution obtained from Topex/Poseidon data and tide gauge from Mazzega and

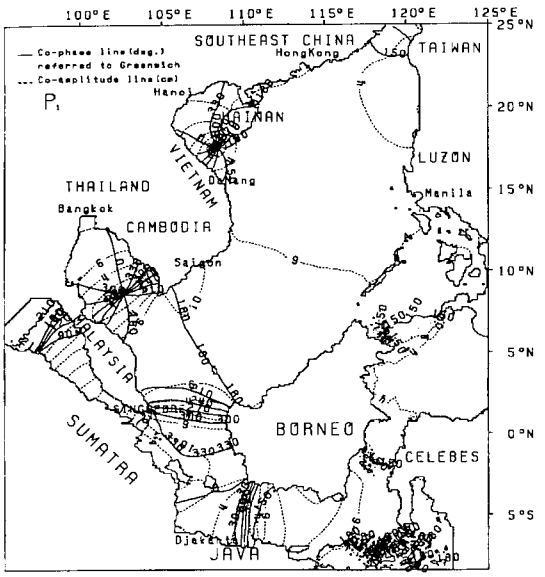

Fig. 9. Computed tidal charts of the P_1 tides for the South China Sea and the Java Sea.

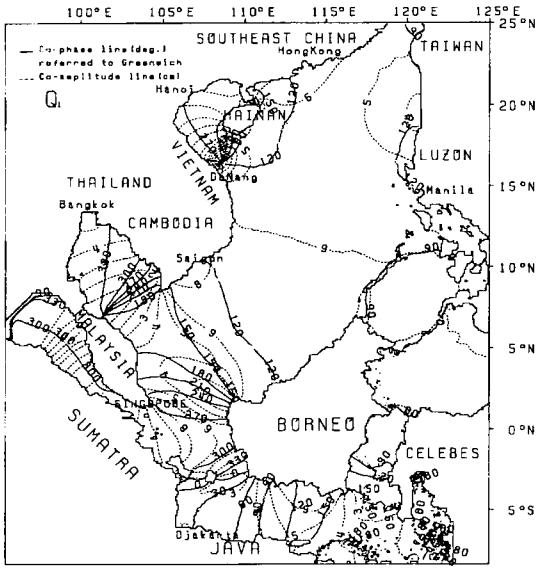

Fig. 10. Computed tidal charts of the Q_1 tides for the South China Sea and the Java Sea.

Berge (1994). But there is positional discrepancy of an amphidromic point in the Gulf of Thailand between T/P derived chart (Mazzega and Berge, 1994) and the model results from Ye and Robinson (1983), Rahman *et al.* (1990), present results indicating resolution of T/P ground tracks are too wide for resolving the narrow shape of the Gulf. Other semi-diurnal charts (S_2, N_2, K_2 tides) show the similar tidal propagation patterns with the M_2 tide but converged cotidal lines around Kepulauan Natuna in the M_2 chart changed to two separated amphidromic system in the S_2 and K_2 tidal charts.

K_1 cotidal chart also show that tides propagate through the two Straits from the Pacific Ocean and the Malacca Strait from the Indian Ocean, but the propagation pattern in the Malacca Strait and the Java Sea is considerably different from the M_2 tidal distribution. There is an amphidromic point at off George Town in the Malacca Strait and the tide from the South China Sea is further propagate into the middle part of the Java Sea. Computed results show that amphidromic points respectively located in the Gulf of Thailand and off northern Vietnam coast are good agreements with Schwiderski's map and result from Ye nad Robinson (1983). An amphidromic point in the Java Sea for the K_1 tide is presented in agreement with Schwiderski's results but other diurnal charts (O_1, P_1, Q_1) did not show an amphidromic point. The O_1 tidal chart shows that an amphidromic point in the Malacca Strait moved close to the western entrance of the Strait.

The numerical experiments show that computed results especially the position of amphidromic points

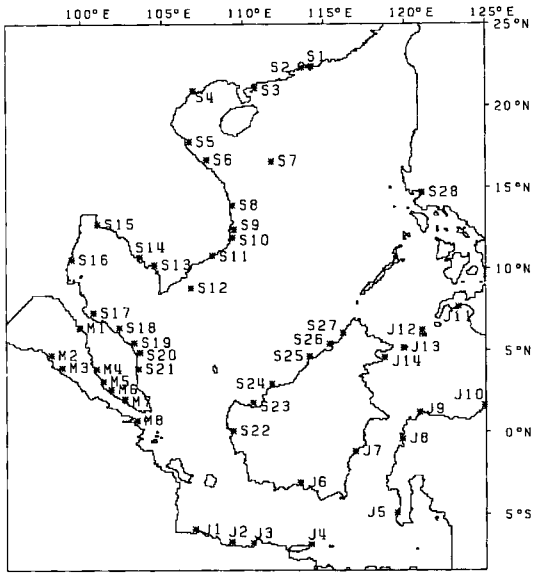

Fig. 11. Selected positions for comparison between model results and coastal gauges.

Table 2. Observed and modeled amplitudes (a_o, a_m: cm) phases (p_o, p_m: deg) of the M_2, S_2, K_1, O_1 tides for the control set of 50 tide gauges.

Tide Gauge	Site	Latitude	Longitude	M_2				S_2				K_1				O_1			
				a_m	a_o	p_m	p_o	a_m	a_o	p_m	p_o	a_m	a_o	p_m	p_o	a_m	a_o	p_m	p_o
S1	HONG KONG	22.28°	114.18°	66.5	40.4	35.8	27.8	30.0	16.2	70.8	58.9	36.2	35.9	179.4	179.2	29.8	28.9	132.5	129.3
S2	MACAO	22.20°	113.55°	76.2	47.4	52.7	48.2	36.3	18.8	87.3	81.4	39.0	37.2	184.8	187.4	31.2	30.9	137.3	137.1
S3	CHANCHIANG	20.95°	110.60°	89.5	78.8	74.1	72.5	49.7	34.9	126.8	120.9	41.5	44.0	208.3	193.8	36.7	39.5	16.10	156.0
S4	HAIPHONG	20.87°	106.67°	2.8	4.4	74.2	219.8	3.1	4.7	293.6	289.7	71.5	63.9	349.6	3.9	82.1	72.9	285.6	297.5
S5	DONG HOI	17.70°	106.47°	30.8	17.6	126.8	161.4	2.7	5.2	194.3	211.3	25.7	21.5	3.5	350.4	35.7	26.9	293.6	293.5
S6	HUE	16.57°	107.62°	21.1	17.7	107.4	112.4	4.3	4.2	140.5	178.5	4.3	3.3	135.1	150.3	5.8	2.3	287.2	260.1
S7	LES PARACELS	16.55°	111.62°	14.8	16.8	48.1	57.9	4.8	7.7	114.7	112.9	29.1	26.8	192.0	185.4	25.0	23.4	144.2	142.1
S8	QUI NHONE	13.75°	109.22°	14.2	17.3	57.4	82.0	5.6	7.0	127.7	127.4	31.3	32.9	190.3	195.5	26.8	28.5	141.9	148.9
S9	NHA TRANG	12.27°	109.30°	14.2	17.2	61.0	81.3	5.8	7.1	129.5	111.4	31.8	32.9	190.5	187.0	27.4	30.1	142.0	139.2
S10	CAM RANH	11.88°	109.20°	14.2	19.5	63.9	89.5	5.9	8.5	131.5	134.6	32.2	34.5	190.1	187.1	27.8	29.4	141.6	146.3
S11	PHAN THIET	10.70°	107.98°	30.6	36.4	162.9	143.9	10.7	15.8	242.1	188.0	7.2	45.3	194.7	182.3	37.2	37.7	144.4	146.6
S12	CON SON IS.	8.68°	106.60°	63.8	79.7	216.9	200.7	26.1	28.4	298.2	261.8	59.8	63.7	220.4	212.7	41.2	44.6	165.2	167.9
S13	HATIEN	10.37°	104.47°	23.8	9.80	180.6	238.9	17.5	1.9	279.1	113.1	20.7	26.2	317.7	320.9	11.0	12.8	283.7	292.1
S14	KOMPONG-SOM	10.63°	103.48°	13.7	11.3	185.3	137.3	9.1	5.5	291.0	193.6	22.7	24.5	15.2	20.6	15.9	18.4	330.6	339.5
S15	SATTAHIP	12.65°	100.88°	18.5	25.7	356.9	271.4	15.5	12.2	112.3	340.9	61.8	59.4	57.2	55.6	38.0	42.0	359.7	7.1
S16	CHUM PHORN	10.45°	99.25°	13.4	12.2	233.7	93.0	9.1	4.0	324.1	205.0	46.7	40.2	68.3	66.0	30.0	26.8	11.8	16.0
S17	SONGKHLA	7.23°	100.62°	19.0	22.6	59.8	82.0	14.9	3.3	148.2	185.0	6.0	5.5	176.5	165.0	6.0	3.7	69.3	93.0
S18	KOTA BAHARU	6.20°	102.27°	20.7	18.0	40.3	55.0	10.3	8.0	130.8	55.0	28.2	29.0	238.3	231.5	13.6	17.0	175.8	196.5
S19	KUALA TRENGGANU	5.35°	103.13°	29.4	26.8	2.5	4.1	11.3	11.0	104.6	49.1	48.2	50.3	246.0	242.0	26.7	29.0	191.9	196.0
S20	KUALA DUNGUN	4.78°	103.43°	36.3	37.7	27.2	6.0	12.6	13.4	99.9	56.0	52.2	57.3	249.7	243.5	30.0	37.2	198.9	198.5
S21	KUANTAN HARBOUR	3.83°	103.33°	51.4	55.7	31.5	31.2	15.7	17.1	102.2	82.3	53.6	51.1	257.2	258.0	31.9	34.7	210.2	215.3
S22	PONTIANAK	-0.02°	109.33°	18.8	12.0	260.7	31.07	9.4	6.0	320.4	322.3	34.3	32.0	14.55	34.0	32.2	24.0	301.1	309.7
S23	KUCHING	1.57°	110.35°	100.7	143.1	227.6	262.1	21.2	40.9	256.3	321.5	45.1	46.3	213.9	231.3	34.4	34.5	160.8	178.4
S24	KUALA IGAN	2.82°	111.70°	41.0	49.0	216.9	228.0	7.8	12.0	212.0	267.0	42.0	42.0	205.8	215.0	34.2	32.0	152.8	154.0
S25	MIRI	4.58°	113.98°	15.2	17.0	73.6	95.0	8.2	8.0	127.3	130.0	34.5	35.0	194.5	199.0	30.8	30.0	144.5	149.0
S26	VICTORIA HAR.	5.27°	115.25°	23.1	27.4	66.7	82.4	9.8	11.8	118.7	128.5	34.8	41.1	193.2	200.1	31.1	33.3	143.7	142.3
S27	KOTA KINABALU	5.98°	116.07°	24.1	23.8	65.8	79.0	9.8	10.4	117.6	113.0	34.5	36.6	193.6	195.0	30.9	30.8	144.3	147.0
S28	MANILA	14.58°	120.97°	20.5	19.1	55.0	54.5	6.2	6.5	107.1	92.6	29.3	29.9	194.4	200.2	25.7	27.8	146.6	147.8
M1	LANGKAWI	6.30°	99.78°	62.7	72.9	120.0	122.4	31.9	41.0	166.6	166.0	5.7	17.8	232.3	236.0	10.5	5.1	30.1	176.0
M2	LANGSA B.	4.50°	98.00°	55.3	56.0	124.2	128.4	27.5	33.0	172.4	172.0	5.4	14.0	250.7	236.3	10.2	6.0	11.8	191.1
M3	BELAWAN DELI	3.83°	98.72°	59.5	61.0	171.2	181.0	26.4	32.0	219.3	219.6	1.9	21.0	346.4	241.6	19.2	4.0	15.4	174.4
M4	TELOK ANSON	4.30°	101.00°	90.6	92.7	245.6	272.0	43.8	64.0	302.5	320.0	14.5	24.4	56.3	269.0	35.5	9.1	21.7	21.0
M5	PORT SWETTENHAM	3.00°	101.38°	113.12	136.2	269.5	282.1	57.6	68.0	325.3	331.2	26.3	18.4	57.3	269.9	46.4	3.4	20.9	60.2
M6	PORT DICKSON	2.52°	101.78°	95.9	81.5	305.4	313.3	49.7	40.5	0.5	2.4	42.3	5.3	58.1	336.5	57.9	15.5	19.1	28.8
M7	MUAR	2.05°	102.57°	82.9	63.4	19.7	25.0	43.9	29.9	76.6	74.0	56.8	13.7	56.8	44.0	64.0	22.9	15.7	29.0
M8	SINGPORE	1.27°	103.85°	101.9	79.6	127.6	87.4	66.4	32.6	181.4	141.1	56.4	29.4	50.2	356.2	51.8	28.3	353.7	304.0
J1	DJAKARTA	-6.10°	106.87°	14.8	5.0	155.6	139.6	2.8	5.0	170.7	86.3	23.6	25.0	44.6	39.4	8.8	13.0	18.9	18.2
J2	TEGAL	-6.85°	109.13°	6.6	9.0	287.1	79.0	13.5	10.0	335.0	345.0	6.2	21.0	42.2	286.0	7.1	5.0	74.9	108.0
J3	SEMARANG	-6.97°	110.42°	16.5	10.0	296.8	46.0	19.3	8.0	331.3	307.2	6.6	22.0	229.6	248.9	10.1	8.0	108.4	126.1
J4	KALIANGET	-7.05°	113.92°	49.9	39.0	111.1	74.0	19.9	19.0	157.6	88.0	40.0	42.0	206.8	179.0	20.2	24.0	148.0	144.0
J5	MAKASSER	-5.15°	119.40°	15.3	8.0	19.5	183.1	15.1	11.0	340.0	315.2	22.9	28.0	179.2	180.9	13.8	17.0	150.9	150.1
J6	MENDAWAI RIVER	-3.28°	113.35°	31.2	42.0	266.0	296.7	18.9	12.0	175.6	216.3	70.7	62.0	223.1	208.0	36.9	34.0	140.5	160.7
J7	BALIK PAPAN B.	-1.27°	116.80°	58.6	59.0	298.7	268.8	45.8	59.0	336.9	337.4	19.7	13.0	163.0	159.5	13.2	13.0	131.6	126.3
J8	DONGGALA	-0.62°	119.73°	52.2	47.0	291.5	271.4	37.3	40.0	329.7	328.5	17.7	22.0	156.7	157.6	12.0	11.0	125.3	110.8
J9	TOLI TOLI B.	1.03°	120.82°	58.7	42.0	285.5	271.2	36.2	35.0	326.0	317.4	15.3	14.0	145.3	164.5	11.5	14.0	116.9	97.7
J10	*MENADO*	*1.50°*	*124.83°*	55.0	56.0	283.1	278.2	31.0	35.0	324.9	322.3	14.9	16.0	140.6	141.5	10.6	16.0	111.8	100.7
J11	MARGOSATUBIG	7.58°	123.17°	58.8	61.9	286.8	282.5	33.5	37.1	327.2	326.7	15.0	14.1	143.9	138.2	10.0	12.2	117.2	118.4
J12	JOLO	6.07°	121.00°	11.0	17.3	325.5	346.6	8.5	10.5	354.8	32.3	26.4	25.8	165.2	195.1	19.5	25.4	128.8	154.9
J13	PORT BONGAO	5.03°	119.77°	49.4	43.1	285.5	267.3	28.7	27.1	325.1	315.5	16.7	17.9	151.0	142.6	12.6	16.0	120.8	119.8
J14	SIMPORNA	4.48°	118.62°	60.1	52.7	284.9	278.0	34.7	25.6	322.4	322.0	15.6	13.4	148.0	159.0	11.5	8.8	120.0	125.0

Table 3. Observed and modeled amplitudes (a_o, a_m: cm) phases (p_o, p_m: deg) of the K_2, N_2, P_1, Q_1 tides for the control set of 50 tide gauges.

Tide Gauge	Site	Latitude	Longitude	M_2				S_2				K_1				O_1			
				a_m	a_o	p_m	p_o	a_m	a_o	p_m	p_o	a_m	a_o	p_m	p_o	a_m	a_o	p_m	p_o
S1	HONG KONG	22.28°	114.18°	10.2	4.4	328.2	57.3	10.6	8.5	16.9	10.3	6.0	11.2	156.6	173.9	7.2	5.4	107.7	105.4
S2	MACAO	22.20°	113.55°	12.2	5.5	342.7	81.7	12.4	9.6	29.7	29.2	6.3	12.1	161.3	184.0	7.5	6.2	112.5	111.5
S3	CHANCHIANG	20.95°	110.60°	15.2	9.5	18.9	121.6	12.0	15.2	48.3	68.1	6.1	14.6	187.7	193.2	8.8	7.6	150.0	151.7
S4	HAIPHONG	20.87°	106.67°	1.4	2.4	298.0	293.1	3.6	0.3	39.3	222.5	15.8	18.4	343.6	354.9	33.8	15.0	265.7	262.1
S5	DONG HOI	17.70°	106.47°	2.9	1.4	49.1	211.9	10.2	3.4	130.8	157.5	6.7	7.1	13.51	349.8	17.0	5.2	281.0	289.2
S6	HUE	16.57°	107.62°	2.1	1.1	55.9	179.0	6.5	3.4	129.6	108.5	3.1	1.1	79.6	149.7	6.1	0.4	300.0	256.3
S7	LES PARACELS	16.55°	111.62°	0.6	2.1	36.4	113.4	2.1	3.2	65.1	57.9	5.1	8.9	162.9	184.8	5.3	4.5	119.9	138.3
S8	QUI NHONE	13.75°	109.22°	0.4	2.1	88.5	122.5	1.8	3.4	79.1	70.4	5.8	10.6	159.7	188.4	5.9	4.9	114.8	130.4
S9	NHA TRANG	12.27°	109.30°	0.4	1.9	102.1	112.1	1.7	3.3	83.7	76.9	6.0	11.0	159.1	186.4	6.0	5.8	115.4	134.9
S10	CAM RANH	11.88°	109.20°	0.4	2.3	107.5	135.3	1.8	3.8	88.5	85.1	6.1	11.5	158.4	186.5	6.1	5.7	115.0	142.0
S11	PHAN THIET	10.70°	107.98°	3.4	4.3	253.0	188.6	8.8	5.6	180.	148.1	9.0	15.1	157.6	181.7	7.8	10.2	117.0	146.8
S12	CON SON IS.	8.68°	106.60°	6.9	7.7	273.3	262.5	15.6	15.4	218.4	196.3	11.1	21.2	172.7	212.1	7.8	8.6	133.7	163.6
S13	HATIEN	10.37°	104.47°	17.8	0.5	265.2	113.7	2.9	1.9	138.1	234.6	2.8	8.7	283.3	320.2	2.2	2.4	267.2	287.7
S14	KOMPONG-SOM	10.63°	103.48°	7.3	2.1	280.6	146.6	3.0	1.9	158.0	125.6	3.9	7.3	334.6	20.3			-	
S15	SATTAHIP	12.65°	100.88°	7.4	3.0	138.8	339.3	4.9	3.8	347.3	238.9	9.5	18.2	4.2	56.2	5.2	7.0	336.2	346.3
S16	CHUM PHORN	10.45°	99.25°	6.2	1.2	41.8	205.0	6.5	2.4	193.0	39.0	7.7	13.4	18.3	66.0	3.9	5.2	342.5	351.0
S17	SONGKHLA	7.23°	100.62°	5.6	0.9	117.2	185.0	4.0	4.3	5.0	30.0	2.1	1.8	86.1	165.0	0.6	0.6	344.0	57.0
S18	KOTA BAHARU	6.20°	102.27°	3.1	2.0	107.9	55.0	6.8	3.0	23.5	18.0	4.4	10.0	169.1	231.5			-	
S19	KUALA TRENGGANU	5.35°	103.13°	4.7	3.0	77.3	49.1	8.8	5.5	31.7	340.1	7.8	16.5	185.3	242.0			-	
S20	KUALA DUNGUN	4.78°	103.43°	5.6	3.7	68.8	56.0	9.7	10.1	39.2	342.0	8.5	19.1	190.8	243.5			-	
S21	KUANTAN HARBOUR	3.83°	103.33°	6.7	6.0	64.6	83.9	12.4	11.4	49.2	5.4	8.4	14.8	198.6	255.4	4.5	6.6	195.2	189.5
S22	PONTIANAK	-0.02°	109.33°	5.0	3.0	274.5	325.9	2.3	3.0	268.7	295.6	7.5	9.0	319.1	34.4			-	
S23	KUCHING	1.57°	110.35°	8.9	12.5	156.4	316.7	19.6	28.1	247.2	239.1	10.0	13.9	167.8	232.5	7.1	6.6	124.6	167.5
S24	KUALA IGAN	2.82°	111.70°	6.0	3.0	144.8	267.0	9.4	11.0	247.5	201.0	9.2	14.0	164.4	215.0	7.4	7.0	120.5	129.0
S25	MIRI	4.58°	113.98°	1.7	2.0	114.4	135.0	1.1	3.0	79.6	86.0	7.2	11.0	159.0	194.0	6.9	6.0	117.6	132.0
S26	VICTORIA HAR.	5.27°	115.25°	1.6	4.3	96.9	113.2	2.6	5.9	74.0	56.0	7.1	14.3	158.3	206.4	7.0	1.2	116.8	264.9
S27	KOTA KINABALU	5.98°	116.07°	1.5	2.7	93.2	117.0	2.9	4.3	71.7	69.0	7.0	10.7	159.1	187.0				
S28	MANILA	14.58°	120.97°	0.8	2.1	78.8	92.4	3.3	3.0	56.7	19.0	5.7	9.7	168.2	191.6	5.9	5.5	119.5	123.1
M1	LANGKAWI	6.30°	99.78°	10.2	11.4	146.6	161.8	6.9	2.6	117.7	116.4	3.7	0.5	91.7	241.8	3.5	1.0	310.4	134.9
M2	LANGSA B.	4.50°	98.00°	8.1	10.0	151.7	172.5	6.2	16.0	127.7	113.9	3.4	5.0	69.5	235.7			-	
M3	BELAWAN DELI	3.83°	98.72°	5.7	9.0	195.1	222.1	6.5	12.0	183.1	174.4	7.2	7.0	68.7	248.0			-	
M4	TELOK ANSON	4.30°	101.00°	12.3	17.4	302.2	320.0	12.6	37.8	253.4	186.0	13.8	7.9	71.1	269.0			-	
M5	PORT SWETTENHAM	3.00°	101.38°	18.4	19.4	317.5	321.8	15.9	25.8	272.7	270.3	17.9	8.4	68.4	273.3	16.2	0.9	300.9	53.4
M6	PORT DICKSON	2.52°	101.78°	16.4	10.0	341.0	0.0	14.0	15.1	306.8	303.5	21.6	3.4	65.0	324.9	21.0	2.4	300.2	1.0
M7	MUAR	2.05°	102.57°	9.9	7.9	60.9	74.0	13.0	12.2	16.8	14.0	22.5	4.6	60.7	44.0			-	
M8	SINGPORE	1.27°	103.85°	29.5	8.8	162.1	139.4	21.1	14.3	117.3	66.9	13.1	8.8	31.5	348.8	20.4	6.1	294.2	265.2
J1	DJAKARTA	-6.10°	106.87°	3.4	2.0	211.9	282.9	2.1	2.0	231.3	91.6	5.4	8.0	9.2	36.8	3.0	3.0	30.3	17.1
J2	TEGAL	-6.85°	109.13°	5.8	3.0	315.6	345.0	4.1	6.0	213.0	37.0	1.9	7.0	20.8	285.0			-	
J3	SEMARANG	-6.97°	110.42°	8.3	4.0	318.7	349.8	3.7	5.0	210.7	9.7	1.2	7.0	137.3	252.3	3.5	2.0	74.8	34.8
J4	KALIANGET	-7.05°	113.92°	7.6	5.0	160.8	88.0	5.3	8.0	107.1	53.0	8.4	14.0	174.0	179.0			-	
J5	MAKASSER	-5.15°	119.40°	4.1	5.0	344.7	354.9	2.9	3.0	226.3	95.7	5.6	11.0	168.3	176.3			-	
J6	MENDAWAI RIVER	-3.28°	113.35°	8.3	8.0	166.9	216.9	9.1	13.0	4.0	273.6	15.3	15.0	168.7	207.3			-	
J7	BALIK PAPAN B.	-1.27°	116.80°	14.4	8.0	340.0	314.0	10.2	8.0	253.6	240.7	4.9	10.0	151.4	119.9			-	
J8	DONGGALA	-0.62°	119.73°	10.2	7.0	332.4	316.2	7.1	4.0	256.0	216.1	4.4	7.0	143.5	170.9			-	
J9	TOLI TOLI B.	1.03°	120.82°	9.6	8.0	326.1	348.0	6.8	6.0	261.4	236.9	4.1	6.0	137.2	206.9			-	
J10	MENADO	1.50°	124.83°	7.6	10.0	328.4	317.0	6.0	9.0	270.4	264.9	3.4	6.0	131.0	147.8	3.3	3.0	49.7	87.4
J11	MARGOSATUBIG	7.58°	123.17°	10.2	10.1	321.7	327.3	6.6	10.0	263.7	278.2	3.5	4.7	139.6	137.5	2.8	2.4	55.3	108.0
J12	JOLO	6.07°	121.00°	1.8	3.4	328.8	31.7	1.2	2.6	251.8	324.5	6.3	8.1	146.9	194.5	4.4	5.2	79.0	137.5
J13	PORT BONGAO	5.03°	119.77°	8.2	7.4	328.0	316.1	5.7	2.4	259.7	126.	4.4	5.9	140.4	141.9	3.4	3.1	61.2	108.4
J14	SIMPORNA	4.48°	118.62°	9.7	8.5	324.0	332.0	7.0	10.1	259.2	237.	3.9	4.6	137.7	157.0			-	

are susceptible to both specified open boundary tide tide-generating potential and loading tides. For the comparision of model results and observations, 50 tide gauge sites (Admiralty Tide Tables, 1992) were selected as shown in Fig. 11. Table 2 and Table 3 show the comparision of observed and calculated amplitudes and phases of the eight major tides for these sites. Fig. 12 and Fig. 13 show tidal ellipses of the M_2 and K_1 tides describing the magnitude and direction of the tidal current distribution. It is seen that M_2 tidal currents are relatively strong in the Malacca Strait and shallow shelf area, but the K_1 diurnal currents are considerably strong in the Gulfs of Tonkin, Thailand and the Java Sea.

The nature of tide in the South China Sea and the Java Sea may be conveniently represented by the use of the Form number (Courtier, 1938). The Form number, F, for a given place is

$$F = \frac{K_1 + O_1}{M_2 + S_2} \tag{8}$$

Fig. 14 show the classified region where diurnal ($F > 1.25$), semi-diurnal ($F < 0.25$) and mixed ($0.25 < F < 1.25$) tides prevail and it is seen that diurnal tide prevail over the South China Sea with semi-diurnal tides in the western part of the Malacca Strait. Mixed tides prevail over the parts of the Gulf of Thailand, the eastern Malacca Strait, middle parts of the Java Sea, the Flores Sea and the Celebes Sea. The amplification of diurnal tides in the South China Sea has been explained by direct astronomical forcing and forced oscillation

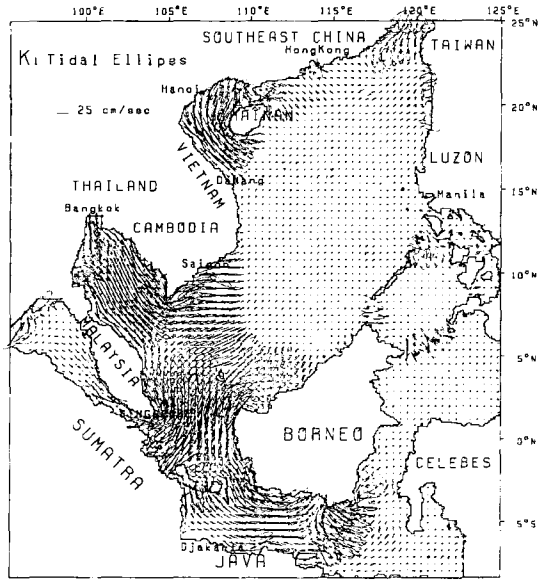

Fig. 13. Tidal current ellipses of the K_1 tides from the model.

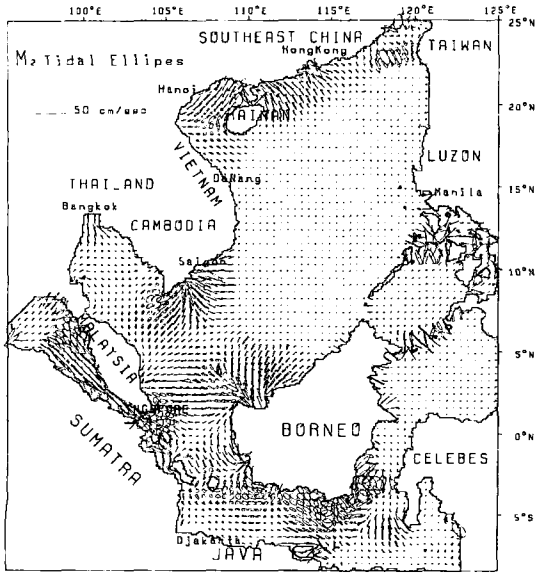

Fig. 12. Tidal current ellipses of the M_2 tides from the model.

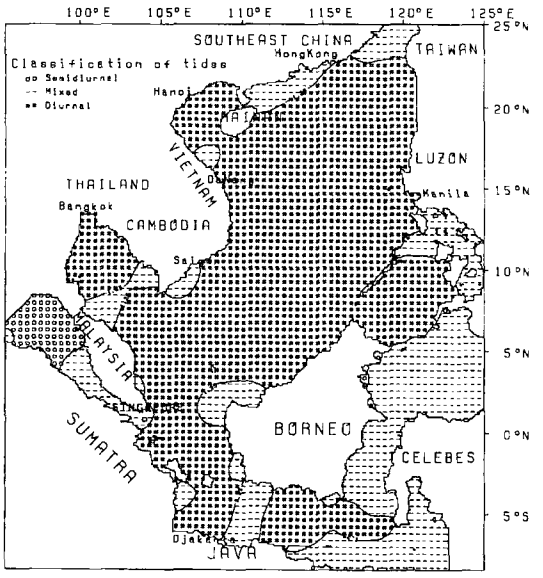

Fig. 14. Classification of tides for the South China Sea and the Java Sea based on model results.

through the ocean connections (Defant, 1962). Williams (1972) showed diurnal amplification in the Gulfs of Tonkin and Thiland as a resonance phenomena. Rahman *et al.* (1990) showed that second and third modes of oscillation period in the Gulf of Thailand is 20 hrs and 12 hrs respectively showing the third modes being corresponds to the M_2 tidal period.

4. CONCLUSIONS

Preliminary result of tides in the Southeast Asian Seas has been presented using the numerical model employed here. By treating the South China Sea, the Java Sea and the Malacca Strait as a whole, tidal dynamics are more reasonably presented by a series of tidal charts. Overall improvement of tidal distribution in the system is being performed based on modified depth fields and open boundary conditions. Improvement of the model employing a refinement of the grid in shallow water is also being performed. Subsequently the developed model also then can be used to study intermediate scale process in the system along with satellite derived sea-level data. Removal of tidal signal from present Topex/Poseidon altimetry by the further improvement of predictive tidal models for this region is necessary. It seems that tides in the Malacca Straits and the Java Sea should be extensively measured to validate the existence of the amphidromic systems.

ACKNOWLEDGEMENT

This work was funded by STAR project of KORDI (Korea Ocean Research and Development Institute).

REFERENCES

Cartwright, D.E., 1978. Ocean tides, Rep. Prog. Phys., pp. 66-708.

Choi, B.H., 1980. A tidal model of the Yellow Sea and the Eastern China Sea, Korea Ocean Research and Development Institute, Report No. 80-02.

Choi, B.H. and Ko, J.S., 1994. Modelling of tides in the East Asian Marginal Seas, *J. of Korean Soc. of Coast. and Oc. Engrs.*, **6**(2), pp. 94-108.

Courtier, A., 1938. Marees. Paris: Service Hydrographique de la Marine, 284p.

Egbert, G.D., Bennett, A.F. and Foreman, M.G.G., 1994. TOPEX/POSEIDON tides estimated using a global inverse model, *J. Geophys. Res.*, **99**(C12), pp. 24821-24852.

Fang, G., 1986. Tide and tidal current charts for the marginal seas adjacent to China, *Chinese J. Oceanology and Limnology*, **4**(1), pp. 1-16.

Flather, R.A. and Heaps, N.S., 1975. Tidal computations for Morecambe Bay, *Geophys. J. R. Astr. Soc.*, **42**, pp. 489-517.

Foreman, M.G.G., Bennett, A.F., Egbert, G.V. and Hagelberg, C., 1992. The removal of tidal elevations from satellite altimeter measurements, *Proc. IX International Conf. on Computational Methods in Water Resources*, Denver, Colorado, USA.

Le Provost, C., Genco, M.L. and Lyard, F., 1994. Spectroscopy of the world ocean tides from a finite element hydrodynamic model, *J. Geophys. Res.*, **99**(C 12), pp. 24777-24797.

Mazzega, P. and Berge, M., 1994. Ocean tides in the Asian semienclosed seas from TOPEX/POSEIDON, *J. Geophys. Res.*, **99**(C12), pp. 24867-24881.

Pingree, R.D. and Griffiths, D.K., 1987. Tidal friction for semidiurnal tides, *Continental Shelf Res.*, **7**(10), pp. 1181-1209.

Rahman, A.A., Isoda, Y. and Yanagi, T., 1990. M_2 tide around west Malaysia, *Memoirs of the Fanculty of Eng.*, Ehime Univ. XII, **1**, pp. 137-147.

Ray, R.D. and Sanchez, B.V., 1989. Radial deformation of the earth by oceanic tidal loading, *NASA Technical Memorandum* 100743.

Roos, A., 1989. IHE course 1989-1990, Lecture notes on tides.

Schrama, E.J.O. and Ray, R.D., 1994. A preliminary tidal analysis of TOPEX/POSEIDON altimetry, *J. Geophys. Res.*, **99**(C12), pp. 24799-24808.

Schwiderski, E.W., 1978. Global ocean tides, Part No.: A detailed hydrodynamical interpolation model, NSWC/DL TR-3866 Naval Surface Weapons Center, Dahlgren, Virginia.

Schwiderski, E.W., 1979. Global ocean tides, Part II: The

semidiurnal principal lunar tide (M2), Atlas of tidal charts and maps, NSWC/TR 81-142.

Thuy, N.N., 1968. Some peculiarities of the formation of tidal phenomena in the South China Sea, *Okeanologia*, **9**(2), pp. 222-230.

Wahr, J., 1981. Body tides on an elliptical, rotating, elastic and oceanless earth, *Geophys. J. R. Astr. Soc.*, **64**, pp. 677-703.

Ye, A.L. and Robinson, I.S., 1983. Tial dynamics in the South China Sea, *Geophys. J. R. Astr. Soc.*, **72**, pp. 691-707.